Available online at www.sciencedirect.com

SCIENCE DIRECT®

Virology 351 (2006) 170–179

VIROLOGY

www.elsevier.com/locate/yviro

Rift Valley fever virus noncoding regions of L, M and S segments regulate RNA synthesis

Nicolas Gauliard [a], Agnès Billecocq [a], Ramon Flick [b], Michèle Bouloy [a,*]

[a] *Institut Pasteur, Unité de Génétique Moléculaire des Bunyaviridés, 25 rue du Dr Roux 75724 Paris cedex 15, France*
[b] *University of Texas Medical Branch, Department of Pathology, 301 University Blvd., Galveston, TX 77555-0609, USA*

Received 1 February 2006; returned to author for revision 3 March 2006; accepted 14 March 2006
Available online 21 April 2006

Abstract

Rift Valley fever virus (RVFV) (*Phlebovirus*, Bunyaviridae) possesses a genome composed of three negative-stranded RNA molecules. Each segment contains 3′ and 5′ noncoding regions with terminal complementary sequences forming a panhandle structure. We showed that transcription–replication of the L, M and S segments is regulated, and we established a minigenome rescue system expressing a CAT reporter to investigate the role of the noncoding regions in this process. The L, M and S segment-based minigenomes were shown to drive bona fide transcription and replication and to express variable levels of CAT reporter, indicating differential promoter activities within the noncoding sequences. In addition, we found a good correlation between the relative promoter strength and the abundance of viral RNA species in RVFV-infected cells. Altogether, these results show that RVFV minigenomes are powerful tools to study transcription and replication and constitute a valuable basis to rescue infectious virus from cDNAs.

Keywords: Minigenome; Reverse genetics; Arbovirus; Bunyaviridae; *Phlebovirus*

Introduction

Rift Valley fever virus (RVFV) belongs to the *Phlebovirus* genus in the Bunyaviridae family (Elliott et al., 2000). It is a pathogen of public health concern in sub-Saharan Africa and Egypt (Meegan and Peters, 1989), which spread to Yemen and Saudi Arabia in 2000 (Anonymous, 2000a,b). RVFV infects humans and ruminants, causing dramatic epidemics/epizootics and leading to major economic losses (Gerdes, 2002; Linthicum et al., 1999; Swanepoel and Coetzer, 1994). RVFV is an arbovirus transmitted by many species of mosquitoes. It persists in the eggs of infected mosquitoes, explaining that the virus can reappear after long inter-epizootic periods, especially after excessive rainfalls during which flooding favors the hatching of eggs and breeding of mosquitoes. The virus contains a tripartite, negative sense RNA genome: the L and M segments code respectively for the RNA-dependent RNA polymerase (L protein) and the glycoprotein precursor, which is co-translationally cleaved, generating the mature envelope glycoproteins G_N and G_C and a nonstructural protein of 14 or 78 kDa, depending of the cleavage site (Giorgi, 1996; Schmaljohn and Hooper, 2001). The S segment utilizes an ambisense coding strategy and contains two open reading frames (ORF), one expressing the nucleoprotein N in the 5′ half of the viral antigenomic-sense molecule (cRNA) and the other encoding the nonstructural protein NSs in the 5′ half of the genomic-sense RNA (vRNA) (Giorgi et al., 1991). A C-rich intergenic region (IGR) separates the two ORFs. All the steps of the viral replication cycle take place in the cytoplasm, maturation and budding occurring in the Golgi apparatus (Schmaljohn and Hooper, 2001).

Like for all the negative-stranded viruses, the RVFV genome is transcribed and replicated only when it is associated with the nucleoprotein and the viral polymerase, forming ribonucleoproteins (RNPs). The viral RNPs are templates for the synthesis of two types of RNAs, mRNAs and antigenomes (cRNAs), the latter ones being the full-length copy of the genome (vRNA). In contrast with genomic and antigenomic RNAs, viral mRNAs

* Corresponding author. Fax: +33 1 40 61 31 51.
E-mail address: mbouloy@pasteur.fr (M. Bouloy).

0042-6822/$ - see front matter © 2006 Elsevier Inc. All rights reserved.
doi:10.1016/j.virol.2006.03.018

are capped with 5′ extensions acquired by cap snatching (Bishop et al., 1983; Patterson and Kolakofsky, 1984) using a mechanism similar to the situation reported for influenza virus (Bouloy et al., 1978; Krug, 1981). Moreover, the mRNAs are not polyadenylated at the 3′ end and are shorter than antigenomes since the viral transcriptase terminates before the 5′ end of the template (Elliott, 1996; Schmaljohn and Hooper, 2001).

In viral infections, the level of expression of each protein is subjected to fine regulations at transcriptional and translational levels. For instance, in *Bunyavirus* infections, the nucleoprotein is one of the most abundant proteins in infected cells, whereas the RNA-dependent RNA polymerase is present in lower amounts. In LaCrosse virus infected cells, regulation was found to occur at the transcriptional level and appears to be cell type dependent (Rossier et al., 1988). Although this was not the case for LaCrosse virus which contains equimolar amounts of each L, M and S segments, different molar ratios of the different genomic segments present in the infecting virus can influence the relative level of protein expression, as it was reported for the related *Phlebovirus* Uukuniemi (Pettersson et al., 1977). Since such data were not available for RVFV, we analyzed the ratio of L, M and S segments in virions and in RVFV infected cells and clearly found that the relative abundance of the three RNA species in infected cells is regulated when compared to the L/M/S molar ratios in the input virus. This study was performed in cells infected by the NSs-deficient Clone 13 in order to eliminate NSs as a possible factor of regulation (Ikegami et al., 2005a). It should be recalled that Clone 13 possesses an NSs which is largely truncated due to an internal deletion and is rapidly degraded by the proteosome pathway (Muller et al., 1995). Among possible factors, we investigated the role of the noncoding regions (NCRs) in transcriptional regulation of the three RVFV RNAs. Each RNA molecule of the tripartite genome contains 3′ and 5′ terminal NCRs composed of a terminal sequence highly conserved within each genus, which is 8 nucleotide-long for phleboviruses, and a more variable internal region specific for each L, M and S segment and having various length, sequence and degree of complementarity between the 3′ and 5′ ends. These 3′ and 5′ sequences are complementary to each other and form a panhandle structure specific for each segment (Elliott, 1996). To address the role of the NCRs in transcription regulation, we used a newly established RNA polymerase I (pol I)-based reverse genetics system expressing a CAT reporter and showed that it drives bona fide transcription and replication from the L, M and S minigenomes. Altogether our data indicate that the relative abilities of the L, M and S genome analogs for transcription–replication were in the order L > S > M, strongly suggesting that the NCRs of each RNA species determine the strength of the promoter activities. Taking into account the molar ratios of the L, M and S segments encapsidated into infectious progeny virions and the size of these RNA molecules, we found a good correlation between the relative strength of the promoters and the relative abundance of the L, M and S RNA species synthesized in infected cells.

Results

Transcription and replication of L, M and S segments are regulated in Clone 13-infected cells

In a first step, we quantified the three viral RNA species incorporated into RVF virions: Clone 13 grown in the presence of [^{32}P]phosphoric acid was purified, its RNA molecules extracted and separated in agarose gel under denaturing conditions (Fig. 1, lane 1). As expected, three bands, L, M and S were observed. The intensity of each band was measured using a PhosphoImager, and the molecular ratio of the L/M/S species was calculated taking into account the size of 6404, 3886 and 1141 nt for the L, M and S segments, respectively. Several preparations of purified virions were analyzed: on average, the molar ratio of L:M:S was 1:3.9:3.9, showing that the M and S segments are almost in equimolar amounts, but the L segment is less abundant. Of note, the three RNA species include small amounts of the antigenomic strand which were incorporated into RVFV particles (unpublished data and Ikegami et al., 2005b). Such a ratio is close to the one (1:4:2) reported for UUK virions (Pettersson et al., 1977).

To evaluate the level of RNA synthesis of the three viral species during viral infection, we infected BHK-21 cells with RVFV Clone 13. Viral RNAs were labeled with [^{32}P] phosphoric acid from 30 min to 7.5 hpi. Actinomycin D was added to the medium to avoid [^{32}P] incorporation in cellular RNAs. This incubation time was chosen because it allows transcription and replication products to accumulate in the cytoplasm, the virus being released in the extracellular medium at later times. Five bands were detected in the gel: the L, M and S RNA species and the N and NSs mRNA (Fig. 1 lanes 2 and 3, the latter being a longer exposure of lane 2). In case of the L or M species, genomes (vRNAs), antigenomes (cRNAs) and mRNAs co-migrated, whereas for the S segment, the N and NSs

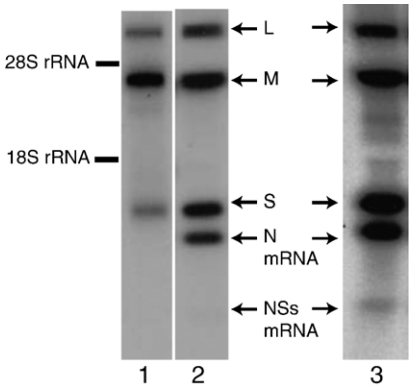

Fig. 1. Analysis of viral RNAs in Clone 13 virions and in infected cells. [^{32}P]-labeled RNAs from purified Clone13 virus produced in the maintenance medium of BSR infected cells and collected at 18 hpi (lane 1) or from Clone 13-infected BSR cells labeled by [^{32}P]phosphoric acid in the presence of actinomycin D from 30 min to 7h30 (lanes 2 and 3) were extracted and separated in a 1.6% agarose gel after denaturation with glyoxal. The gel was dried and exposed to X-ray film. Lanes 2 and 3 represent two exposures of the same gel. The intensities of the bands were quantified.

mRNAs were easily separated because of their size difference. The N and NSs mRNAs were estimated, respectively, to be approximately 850 and 390 base-long from their migration relative to size markers in denaturing gels.

To determine the level of transcription and replication relative to each species, we quantified the intensity of L, M and S RNAs, including vRNA, cRNA and mRNA, synthesized in Clone 13-infected cells (Fig. 1, lane 2). The NSs subgenomic mRNA, which is barely detectable, was not quantified because it contributes only for a negligible proportion. In case of the L and M segments, the unique band represents the transcription and replication activity since the genome, antigenome and mRNA comigrate. For the S segment, the intensities of the full-length molecules and the N mRNA were added. Based on the respective intensities of the bands and their size, we calculated that the synthesis of one molecule of L RNA was associated with 2.8 molecules of M RNA and 12.3 molecules of S RNA, the latter ones being composed of 6.3 of full-length S RNA, 6.0 of N mRNA and minor amounts of subgenomic NSs mRNAs.

These results show that the level of each RNA species is regulated in RVFV-infected cells, in a context where NSs is inefficient. The proportion of S RNA species is higher in infected cells compared to virions, M RNA species is lower in infected cells than in virions, and the L species is the least abundant. It is possible that, as described for other bunyaviruses (Barr et al., 2003; Flick et al., 2004; Kohl et al., 2004a; Lowen and Elliott, 2005; Lowen et al., 2005), promoters for transcription–replication of L, M and S RNA species have different strength and regulate the levels of RNA transcription–replication. Thus, we established RVFV minigenome rescue system and investigated if the relative levels of L, M and S RNA synthesis could be due to the strength of their promoter contained within the NCRs.

Development of RVFV L, M and S segment-based minigenomes

To address the role of the NCRs in transcription regulation, we utilized a minigenome system in which the CAT reporter gene ORF was cloned in the noncoding (antisense) orientation between the 5′ (110, 271 and 38 nt) and 3′ NCRs (18, 20 and 34 nt) of the genomic L, M or S segment (vRNA). In the different strains completely sequenced today, Clone 13, MP12 and ZH548, the NCR sequences are fully conserved. In the case of the S segment, the Clone13 NSs and intergenic sequences (249 nt plus 82 nt) were included to mimic the S segment more closely and because the IGR contains a site for transcription termination. This system will allow comparison of the control elements located within NCRs from each genome analog without interference of various RNA sequences and sizes, since the templates have approximately the same size and express the same reporter protein.

Previous reports indicated that the reconstitution of the RVFV transcription complex requires the L and N proteins (Ikegami et al., 2005a; Lopez et al., 1995). Therefore, the L and N proteins were expressed in BSR cells after transfection of pTM1-L and pTM1-N, in which the respective ORFs were cloned downstream of the T7 promoter and the IRES of EMCV of the pTM1 plasmid, allowing protein expression via cap-independent translation (Elroy-Stein et al., 1989). T7 RNA polymerase was provided by co-transfection of pCMV-T7pol, a plasmid carrying the ORF of the T7 RNA polymerase under the CMV promoter (Radecke et al., 1995).

In the system we developed here, the minigenomes were expressed from Pol I-based plasmids pLgCAT, pMgCAT or pSC13gCAT, similar to those already described for other bunyaviruses (Flick and Pettersson, 2001, Flick et al., 2003a,b, 2004). Plasmid pRF108 containing the promoter and terminator of the murine RNA polymerase I system served as a cloning vector. To control transfection efficiencies and to normalize CAT activities, pTM1-$Luc_{firefly}$, a plasmid encoding the reporter firefly luciferase under T7 polymerase promoter and the EMCV IRES was also constructed. Experiments were carried out to determine the amounts and ratios of the plasmids to obtain the optimal level of CAT activity. The conditions retained are the following: 0.25 μg of pTM1-L and 0.5 μg of pTM1-N together with 1 μg of pLgCAT and 2 μg of pCMV-T7pol were transfected (data not shown). Transcription of the three RVFV minigenomes mediated by the viral complex was then monitored in a time course experiment by enzymatic CAT assay using LgCAT, MgCAT or SC13gCAT as a template. Fig. 2A illustrates the data obtained after transfection of pLgCAT. Similar data were obtained for M and S segment-based minigenomes, and transfection efficiency was similar for each time point as monitored by the pTM1-$Luc_{firefly}$ (not shown). As expected for these RNA molecules which possess a CAT ORF in the noncoding orientation, no activity was found in the absence of N and/or L (Fig. 2A, lanes 1–3). In contrast, in cells expressing L and N, CAT activity was detected as soon as 12 h post-transfection (lanes 5–10) indicating that L and N are the minimal *trans*-acting viral factors required for transcription, which confirms previous work (Lopez et al., 1995). CAT activity was found to increase over time until 48 h, finally reaching a plateau (Fig. 2A).

The L, M and S minigenomes are transcribed and replicated like authentic viral genomes

To validate the transcription–replication system, we verified that these artificial templates are also efficient for replication like the authentic viral molecule. The replication activity was demonstrated by Northern blot analyses. Minigenomes, miniantigenomes and the mRNAs were analyzed using probes annealing to the CAT sense or antisense sequences (Figs. 3A and B). In cells transfected with each genomic plasmid and in the absence of N protein (or L, not shown) expression, a probe against antisense CAT detects the primary products of the cellular pol I transcription (Fig. 3B, lanes 2, 4, 6). In the presence of L and N proteins, genomic CAT RNAs were detected in higher amounts (Fig. 3B, lanes 3, 5, 7), demonstrating that the genome analog was amplified and, therefore, that replication occurred.

We verified also that the transcriptase activity synthesizes mRNAs which are truncated at their 3′ ends relative to the

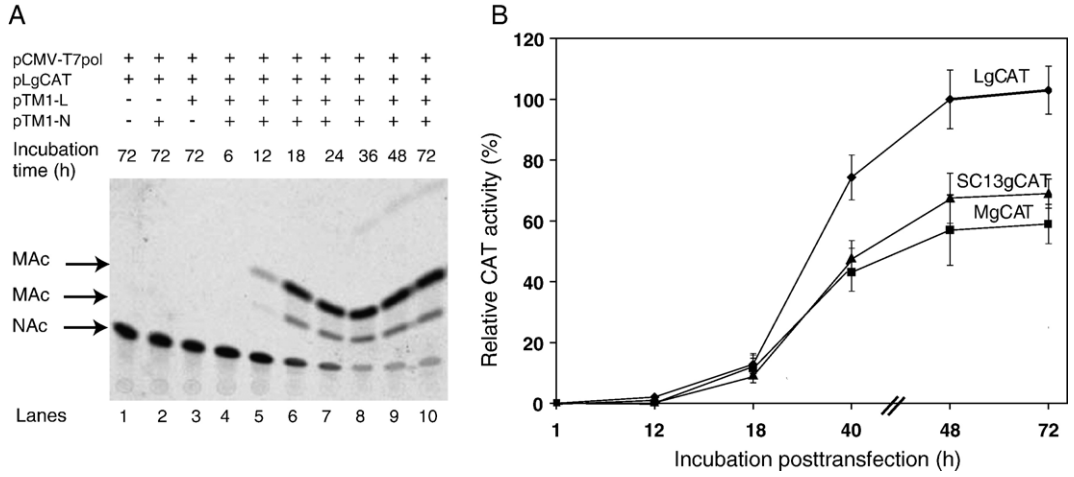

Fig. 2. Detection and quantification of CAT activity mediated by CAT minigenomes. (A) Kinetics of CAT expression recovered from LgCAT minigenome. BSR cells were transfected with 2 μg of pCMV-T7pol, 1 μg of pLgCAT, 0.25 μg of plasmid pTM1-L and 0.5 μg of pTM1-N. In the negative controls, one or both protein expression plasmids were omitted. Cells were incubated at 37 °C for 6 h to 48 h post-transfection, CAT activity was assayed and revealed by thin layer chromatography. The chromatogram is shown after exposure on a screen (STORM). MAc: monoacetylated chloramphenicol, NAc: nonacetylated chloramphenicol. (B) Comparison of CAT expression from the L, M and S RVFV minigenomes. Experiments were carried out as described above and the percentage of monoacetylated chloramphenicol was estimated. CAT activity from LgCAT at 72 h was considered as 100%.

antigenomes, like the authentic viral molecules (Elliott, 1996). Northern blotting using a probe detecting CAT in the sense orientation was performed to analyze the antigenome analogs and the CAT mRNAs (Fig. 3A, lanes 3, 5, 7). As expected, no background was observed in the absence of N and L protein expression (Fig 3A, lanes 2, 4 and 6). In the case of L segment-based minigenomes, when L and N were expressed, it was not possible to distinguish antigenome-like molecule and CAT mRNA from their migration in the agarose gel, whereas two bands were detected in cells transcribing the M and S minigenomes (Fig. 3A). Taking the viral context as a reference, we assumed that the slow migrating band corresponds to the antigenome analog, and the faster migrating one corresponds to the CAT mRNA. For the authentic M mRNA, the 3′ end was mapped (Collett, 1986) and located at some 110 nt before the end of the template. The difference in mobility between the two CAT RNAs suggests that termination occurs at the expected signal in the M analog. Using size markers and the three segment-based CAT minigenomes, we estimated the fast migrating RNA expressed from SC13gCAT template to be approximately 780 nt in length. This is in agreement with the fact that this CAT mRNA contains a 5′ capped extension of 10–18 bases, the 5′ antigenomic NCR of S (38 nt), the CAT gene (661 nt) and most of the IGR, suggesting that the transcriptase terminates after copying most of the IGR, like in the case of the N mRNA in RVFV infected cells. Additionally, since the SC13gCAT template is ambisense, we checked by Northern blot analysis if the NSs mRNA was transcribed. Fig. 3C shows that although in small proportion, the NSs mRNA was synthesized, and it co-migrated with the NSs mRNA from Clone 13-infected cells. Altogether, these data showed that the termination signals for both mRNAs are present in the IGR, and that the minigenomes are bona fide templates for transcription and replication.

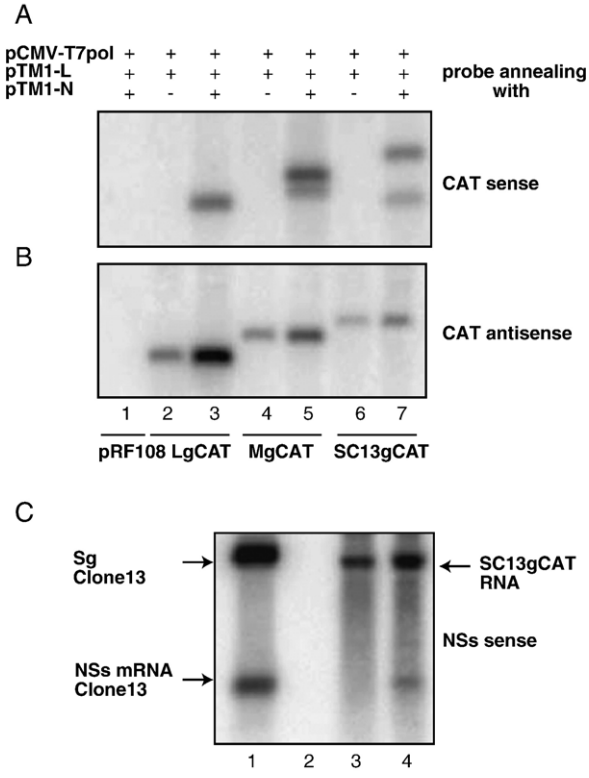

Fig. 3. Northern blot analysis of BSR cells transfected with the set of plasmids to reconstitute RVFV polymerase and the minigenome pLgCAT (A and B, lanes 2 and 3), pMgCAT (A and B, lanes 4 and 5) and pSC13CAT (A and B, lanes 6 and 7 and C, lanes 3 and 4) or the plasmid vector pRF108 (A and B, lanes 1). Negative controls in which pTM1-N is lacking are shown in panels A and B, lanes 2, 4 and 6 and in panel C, lane 3. RNAs from BSR cells, uninfected (C, lane 2) or infected with Clone 13 (C, lane 1) were analyzed as a control. The probes detected the CAT sense (A), antisense (B) or the NSs sequence in the sense orientation (C).

The NCR are responsible for regulation of viral RNA transcription–replication

When we compared CAT expression from the genomic L, M and S minigenomes, we found that CAT activity was 1.7 times stronger when expressed from pLgCAT than from pMgCAT and 1.6 times stronger than from the pSC13gCAT (Fig. 2B). In other words, the relative efficiency of the promoters was 100%, 59% and 64% for the L, M and S RNA species, respectively. These ratios did not change over the course of the experiment. We verified that the truncated NSs of Clone 13 has no effect on viral transcription by using a pSC13mgCAT (m for mutated) in which the NSs ATG start codon was mutated into a TGA codon: CAT activity recovered from this plasmid gave similar results compared to the pSC13gCAT plasmid (not shown).

The relative transcription–replication activity in infected cells seems in contrast with the results obtained from the minigenome system: the transcription–replication activity of the L molecules is the lowest in infected cells, whereas the L promoter assessed by the minigenome comparison is the strongest. This is, however, an apparent paradox since in the minigenome analysis, the three templates are of similar size, whereas the sizes of the authentic molecules are quite different. Theoretically, the efficiency for RNA synthesis of the L, M and S species must be proportional to the strength of the promoter (100%, 59% and 64%, respectively) and inversely proportional to the length of the L, M and S molecules, i.e., 6404 nt, 3886 nt and 1141 nt, respectively. Thus, the size correction factor is 1 for L, 1.6 (i. e. 6404: 3886) for M and 5.6 (i. e. 6404: 1141) for S and the theoretical molar ratio of the RNA species in infected cells must be 1 for L, 0.97 (i. e. 0.59 × 1.6) for the M species and 3.55 (i. e. 0.64 × 5.6) for the S species. This theoretical calculation shows that the S species takes advantage because of its small size, but it assumes also that the three RNA species are in equimolar ratios. Thus, the proportion of the L, M and S species in infected cells have to be corrected, knowing that the relative amounts of the input RNPs from the Clone 13 infecting virus are 1 for L, 3.9 for M and 3.9 for S (see Fig 1). When this parameter was introduced, the calculation leads to the following theoretical molar ratio in infected cells: 1 for L, 3.8 for M and 13.8 for S. These values were close to those observed in infected cells, which are 1:2.8:12.3. Therefore, these results strongly suggest that the *cis*-acting elements present in the NCRs of each minigenome control the level of transcription–replication in a manner similar to the situation encountered in RVFV-infected cells.

Discussion

In this study, we described a Pol I-driven RVFV minigenome rescue system and showed that it is functional for the reconstitution of virus-like RNPs fully active for transcription and replication. The three types of transcription products were synthesized, and the ratios between mRNA and antigenomes (cRNAs), at least those derived from the S segment-based minigenomes (Fig 3A, lane 7) or the S segment in RVFV-infected cells (not shown), were similar, indicating that transcription–replication was regulated similarly in both systems. The mRNAs are likely to possess 5′ capped extension since expression of the recombinant L protein was shown to carry out cap snatching (Lopez et al., 1995). In addition, CAT mRNAs expressed from M and S segment-derived minigenomes terminate at a signal located in the 5′ NCR or in the IGR, respectively. The presence of the IGR in the S segment-based minigenome plasmid is important to assess the level of expression since an S CAT template lacking the IGR (SgCAT) was found to be much less active than SC13gCAT (data not shown). Similar results were observed with UUKV minigenome (Flick et al., 2004). Likely, the SgCAT template lacking the transcriptase termination signal generates CAT mRNAs containing the complete 5′ and 3′ NCRs which can form a panhandle structure and impede efficient translation. The termination signal present in the M segment …GGGGTGGTGGGG… (Collett, 1986) is likely recognized by the reconstituted complex (Fig 3A, lane 5). The question of the transcription termination site has to be addressed for the RVFV L mRNA because such a sequence is not present in the 3′ NCR of the L segment, and no termination site was determined. Considering that the transcription products from the segment-derived minigenome migrated as a unique band, it could be that the L mRNA and the antigenomes (cRNA) have the same size, as it occurs for the L mRNA of Sin Nombre (Hutchinson et al., 1996).

The minigenome rescue system allowed assessing the relative promoter efficiencies of the L, M and S minigenomes by measuring CAT activities. The validity of assessing promoter strength by the reporter activity of genome analogs was already raised for Bunyamwera virus minigenome, and an excellent correlation was found between reporter gene activity and direct labeling of the minigenome analogs (Barr et al., 2003; Kohl et al., 2004a). Because of the similarity of the systems, this should be true also for the RVFV minigenomes. A possible bias could occur if CAT expression is influenced by the context of the initiating AUG (Kozak, 2002). In all the minigenomes, position +4 is the same, due to the CAT ORF and position −3 depends on the sequence of the NCR. For RVFV L and S minigenomes, position −3 is an A and therefore is optimal, whereas for the M minigenome, position −3 is a U, leading to a less favorable translation efficiency. On this basis, one could consider that the activity resulting from the M minigenome is underestimated. However, the AUG context for CAT expression might not have a significant effect since for Bunyamwera and Uukuniemi virus minigenomes, essentially no difference in CAT activity was found when the translational context was changed to be optimal (Flick et al., 2004; Kohl et al., 2004a). Therefore, it is reasonable to consider that evaluation of CAT activities represent a valid method to assess the efficiency of the L, M and S promoters.

Altogether, our results indicated that the NCRs contain the L, M and S promoters, the strength of which is in the order L > S > M, whereas the level of genome segment transcription and replication in infected cells is almost in the opposite order S > M > L. Theoretically, this can be explained merely by the fact that the larger the molecule to transcribe and replicate, the

stronger the promoter has to be. However, in similar studies carried out with the related *Phlebovirus* UUKV and the orthobunyavirus Bunyamwera, the M segments were shown to have the highest transcription–replication ability, followed by the L and S segments (Barr et al., 2003; Flick et al., 2004; Kohl et al., 2004a). Although it is beyond the scope of this paper to elucidate the mechanism leading to differential RVFV promoter activities, it is interesting to speculate on the elements present in the NCR and possibly involved in regulation. Several factors or elements have to be considered, among which sequence variations and structures. Except for the extreme terminal nucleotides conserved among segments and viruses of the same genus, the remaining sequences of the NCRs are specific for each segment. Fig. 4 illustrates the sequence and potential structure of the L, M and S RVFV CAT minigenome panhandles predicted using the *M*-fold programme (Zucker et al., 1999). The difference of promoter strength could be due to a particular sequence and/or structure within the NCRs. These elements could influence the binding of the L protein and/or its capacity to initiate transcription as well as the ability of the nucleoprotein to bind RNA. In influenza virus promoter, the 5′ sequence of the panhandle determines the binding of the polymerase, whereas the 3′ sequence influences the transcription initiation (Li et al., 1998). Also, it appears that increased complementarity between the 3′ and 5′ sequences influenced the efficiency of the transcriptase. Indeed, in the case of Bunyamwera virus, it was shown that the 3′ and 5′ NCRs do not act independently but rather cooperate to form a functional promoter and a minimal length of base-paired ends, up to nt 15 or 16, is required for functionality (Barr and Wertz, 2004). To some extent, this was shown also for UUKV minigenome (Flick et al., 2004), and it is suggested for RVFV by the fact that chimeric CAT constructs in which the 5′ NCR of the M segment was associated with the 3′ NCR of the L or S segment were not functional for transcription–replication (not shown). Additionally, data reported by Kohl et al. indicated that a point mutation at nucleotide 16 in Bunyamwera virus S segment introducing a loop structure in the panhandle and a decrease in free energy was responsible for a strong increase of N mRNA transcription (Kohl et al., 2003). In terms of secondary structure, a loop is predicted within the RVFV S panhandle, next to the stem formed by the terminal 8 base-paired nucleotides (Fig 4). This is a major difference with the structure predicted for UUKV S segment which might explain that the promoter of UUKVS segment is the weakest of the three genomic segments (Flick et al., 2004). Mutational analysis would help to elucidate this question by disrupting the loop structure in the RVFV S minigenome and introducing mutations to generate complementary sequences. Moreover, the 5′ NCRs of the L and M segments are long, and only the base paired structures of RVFV are shown in Fig 4. Similar structures are predicted for the L and M panhandles of UUKV, with a loop in the L segment and a bulge in the M one (not shown). However, the L segment promoter is stronger within the RVFV genome, whereas this is the M one in the UUKV genome. Why these differences exist among these two viruses is not clear. Particular sequences and structures present downstream of the panhandle must be important to modulate the promoter. Mutational studies using the minigenome system will be necessary to identify the *cis*-acting elements present in each NCR affecting the strength of the RVFV promoter. One should also keep in mind that, as described for Bunyamwera virus (Kohl et al., 2004b), relative promoter strength might depend on the cell type in which the minigenome is functioning and suggesting that cellular factors might be involved.

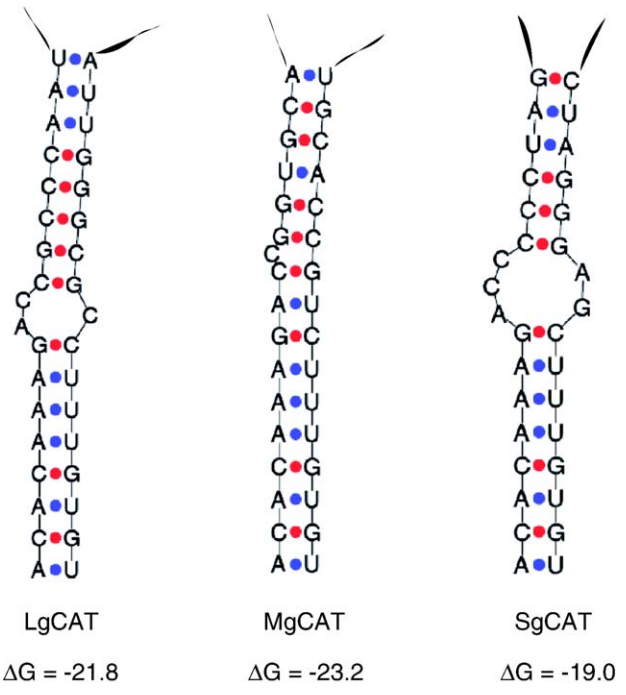

Fig. 4. Panhandle structures predicted for the L, M and S CAT minigenome. The *M*-fold programme was used to determine the secondary structures of the full-length L, M and SC13 CAT minigenomes. Only the terminal regions forming panhandle between 3′ and 5′ ends are shown.

Material and methods

Cells lines and virus strains

BSR cells were grown in Glasgow's modified Eagle's medium (GMEM, Gibco-BRL) supplemented with 5% fetal calf serum, 10 IU of penicillin/ml and 10 μg of streptomycin/ml. BHK-21 cells were grown in GMEM supplemented with 5% fetal calf serum, 5% tryptose phosphate broth, 10 mM of HEPES, 10 IU of penicillin/ml and 10 μg of streptomycin/ml.

RVFV Clone 13 and MP12 were grown by infecting Vero E6 cells at a low multiplicity of infection (MOI) of 0.01. The maintenance medium, Dulbecco's medium containing 2% fetal calf serum and antibiotics was collected at 72 hpi and stored at −80 °C.

Construction of plasmids

The sequences representing the ORFs of N and L proteins were amplified by RT-PCR from MP12 RNA extract and cloned into the pTM1 plasmid, yielding pTM1-N and pTM1-L. The PCR primers used for plasmid constructions are shown in

Table 1. Plasmid pRF108 (Flick and Pettersson, 2001) was used for expression of RVFV segment-like molecules under the control of the murine RNA pol I promoter (Neumann et al., 1994; Zobel et al., 1993). The 5′ and 3′ NCR cDNAs of L, M and S RVFV MP12 were inserted between the rRNA gene promoter region (−251 to −1 relative to the 45 S pre-rRNA start point) and the rDNA terminator sequence (+571 to +745 relative to the 3′ end of the 28 S rDNA), in genomic (g) or antigenomic (ag) orientation for vRNA and cRNA transcription, respectively. The pLgNC and the pMgNC were constructed using the primers RVFL5NC/RVFL3NC and RVFM5NC/RVFM3NC, respectively. The RVFL3NC and the

Table 1
Names and sequences of the primers used for the plasmid construction

Primer	Sense	Sequence	Plasmid
VFL5NC	Forward	AATC**GTCTCT**AGGT*ACACAAAGACCGCCCAATATT* ***BsmBI*** ***5′ RVFV L-NCR (vRNA) nts 1 to 21***	pLgNC
RVFL3NC	Reverse	AAT**CGTCT**CGGGG*ACACAAAGGCGCCCAATCAT***GTCTTC**GGT— ***BsmBI*** ***3′ RVFV L-NCR (vRNA)*** ***Bbs I*** —ACCTCGA**GAAGAC**AG*GACCAGTAAGCAAAGTCAGGCTTAG* ***Bbs I*** ***5′ RVFV L-NCR(vRNA) nts 121 to 97***	
CATL5NC	Forward	AAT**GAAGAC**GGAATC*ATGGAGAAAAAAATCACTGG* ***Bbs I*** ***CAT N-terminus***	pLgCAT
CATL3NC	Reverse	AAT**GAAGAC**GGGGTC*TTACGCCCCGCCCTGCCACTC* ***Bbs I*** ***CAT C-terminus***	
RVFLCAT5NCag	Forward	AAT**CGTCTC**TAGGT*ACACAAAGGCGCCCAATCAT* ***BsmBI*** ***5′ RVFV L-NCR (cRNA)***	pLagCAT
RVFLCAT3NCag	Reverse	AAT**CGTCTC**GGGGA*CACAAAGACCGCCCAATAT* ***BsmBI*** ***3′ RVFV L-NCR (cRNA)***	
RVFM5NC	Forward	AAT**CGTCTC**TAGGT*ACACAAAGACCGGTGCAACTTCAAAGAG* ***BsmBI*** ***5′ RVFV M-NCR(vRNA) nts 1 to 28***	pMgNC
RVFM3NC	Reverse	AAT**CGTCTC**GGGGA*CACAAAGACGGTGCATTAA*AT**GTCTTC**G— ***BsmBI*** ***3′RVFV M-NCR (vRNA)*** ***Bbs I*** —GTACCTCGA**GAAGAC**AG*ATCAGTGCGTGTAAAAGTCATATG* Xho I ***Bbs I*** ***5′ RVFV M-NCR(vRNA) nts271 to 248***	
CATM5NC	Forward	AAT**GAAGAC**GGTTAA*ATGGAGAAAAAAATCACTGG* ***Bbs I*** ***CAT N-terminus***	pMgCAT
CATM3NC	Reverse	AAT**GAAGAC**GGTGAT*TTACGCCCCGCCCTGCCACTC* ***Bbs I*** ***CAT C-terminus***	
RVFMCAT5NCag	Forward	AAT**CGTCTC**TAGGT*ACACAAAGACGGTGCATTAAATG* ***BsmBI*** ***5′ RVFV M-NCR(cRNA)***	pMagCAT
RVFMCAT3NCag	Reverse	AAT**CGTCTC**GGGGA*CACAAAGACCGGTGCAACTTC* ***BsmBI*** ***3′ RVFV M-NCR (cRNA)***	
RVFS3NC	Forward	AAT**CGTCTC**GGGGA*CACAAAGCTCCCTAGAGATACAAACACT*A ***BsmBI*** ***3′ RVFV S-NCR(vRNA)*** —*TTACAATA*AT**GTCTT**CGGTACCTCGA**GAAGAC***AGGATAACTT*— ***Bbs I*** Xho I ***Bbs I*** —*GATAAGCACTAGGGGGTCTTTGTGT*ACCTA**GAGACG**ATT— ***5′ RVFV S-NCR (vRNA)*** ***BsmB I***	pSgNC
RVFS5NC	Reverse	AAT**CGTCTC**TAGGT*ACAC* ***BsmBI*** ***5′ RVFV S-NCR (cRNA)***	
CATS5NC	Forward	AAT**GAAGAC**GGAATA*ATGGAGAAAAAAATCACTGG* ***Bbs I*** ***CAT N-terminus***	pSgCAT
CATS3NC	Reverse	AAT**GAAGAC**GGTATC*TTACGCCCCGCCCTGCCACTC* ***Bbs I*** ***CAT C-terminus***	
CATSins	Reverse	AAT**CGTCTC**TTATCCC**GTCTTC**GTACCTCGA**GAAGAC***GGTTACGC*— ***BsmB I*** ***Bbs I*** Xho I ***BbsI*** —*CCCGCCCTGCCA* ***CAT C-terminus***	/pSinsgCAT
CATIR3	Forward	AAT**CGTCTC**TGTAA*GTGGCTGCCCAGGGGGTT* ***BsmB I*** ***3′ end of Intergenic Region (vRNA)***	
NSsC13	Reverse	AAT**CGTCTC**TTATC*ATGGATTACTTTCCTG* ***BsmB I*** ***NSs N-terminus***	pSC13gCAT
NSsC13mut	Reverse	AAT**CGTCTC**TTATC*TAGGATTACTTTCCTG* ***BsmB I*** ***NSs N-terminus (ATG changed to TAG)***	/pSC13mgCAT
RVFSCAT5NCag	Forward	AAT**CGTCTC**TAGGT*ACACAAAGCTCCCTAGAGAT* ***BsmBI*** ***5′ RVFV S-NCR (cRNA)***	pSagCAT /pSC13agCAT
RVFSCAT3NCag	Reverse	AAT**CGTCTC**TGGGA*CACAAAGACCCCCTAGT* ***BsmBI*** ***3′ RVFV S-NCR (cRNA)***	/pSC13magCAT

RVFM3NC primers contain the complete 3′ NCR of L or M, a BbsI-XhoI-BbsI cloning site and the last nucleotides of the 5′ NCR of L or M. The pSgNC was constructed using the oligonucleotide RVFSNCfull containing the whole 3′NCR of the S segment followed by a BbsI-XhoI-BbsI cloning site and the complete 5′ NCR. A double-stranded DNA product was synthesized by the Klenow polymerase using the RVFSNCstart primer and the oligonucleotide RVFSNCfull. The CAT reporter gene was then cloned in antisense orientation between the NCRs using the primer sets CATL5NC/CATL3N to yield the pLgCAT plasmid or CATM5NC/CATM3NC for the pMgCAT plasmid or CATS5NC/CATS3NC for the pSgCAT plasmid. Plasmid pSinsgCAT containing the NCRs of the S segment flanking a BbsI-XhoI-BbsI sequence and the CAT gene was constructed by inserting the PCR product obtained using CATS5NC/CATSins primers, into the pSgNC plasmid. Primer CATSins contains BbsI-XhoI-BbsI cloning sites which allow insertion of any sequence between the 5′ S NCR and the CAT gene. The pSC13gCAT plasmid was constructed by inserting the NSs gene and the 82 base long IGR of Clone13 using CATIR3/NSsC13 primers into pSinsgCAT. The same method was used to generate the pSC13mgCAT plasmid, with CATIR3/NSsC13mut primers, which contains the NSs gene with the initiating ATG mutated into TAG.

Plasmids pLagCAT, pMagACT, pSC13agCAT, pSC13mag-CAT and pSagCAT, transcribing respectively the viral L, M and S cRNA antigenome (ag) analogs were constructed using RVFLCAT5NCag/RVFLCAT3NCag primers and pLgCAT template, RVFMCAT5NCag/RVFMCAT3NCag primers and pMgCAT template, and RVFSCAT5NCag/RVFSCAT3NCag primers and pSC13gCAT or pSC13mgCAT or pSgCAT templates, respectively. All the plasmids were checked by sequencing.

DNA transfection

BSR cells were grown in 6-well plates up to 70–80% of confluency. Before transfection, culture medium was replaced by OptiMEM medium (Gibco), then cells were transfected by DOTAP liposomal transfecting agent (Roche) according to manufacturer's specifications. Cells were incubated for 6 to 72 h at 37 °C. Four hours post-transfection, OptiMEM medium was removed and replaced by GMEM containing 5% fetal calf serum.

CAT assay

BSR cell monolayers were washed with cold phosphate-buffered saline (PBS), harvested by scraping into PBS and recovered by centrifugation. The cell pellet was resuspended in 50 µl of 0.25 M Tris, pH 7.5. Cells were lysed by three cycles of freezing and thawing. Cell lysate was clarified by centrifugation (9000 × *g*, 4 °C). For the enzymatic assay, 7 µl of cell extract was mixed with 86 µl of 0.3 M Tris pH 7.5, 16 µl of 4 mM acetyl coenzyme A (Roche) and 2 µl of [^{14}C] chloramphenicol (10 nCi, 50–62 mCi/mmol, Amersham) and incubated for 40 min. For quantification of CAT activities, the incubation times and the amount of lysates were adjusted so that the reaction did not produce di-acetylated chloramphenicol but only the monoacetylated form, indicating that the synthesis was carried out in a linear range. The reaction products were separated by thin-layer chromatography (TLC plate, 20 × 20 cm; Silica Gel 60, Merck) developed with 19:1 chloroform: methanol. Mono- and nonacetylated [^{14}C]chloramphenicol were visualized by autoradiography using STORM 820 (Molecular Dynamics), and CAT activity was quantified as the proportion of monoacetylated chloramphenicol using ImageQuant (Molecular Dynamics).

Analysis of RNA

Purification and analysis of ^{32}P-labeled virion RNAs

Four 10-millimeter dishes of BHK-21 were infected with Clone 13 RVFV at an MOI of 1. [^{32}P]phosphoric acid (20 µCi/ml) (MP Biomedicals Inc.) was added to the medium 2 h later, and cells were harvested at 18 hpi. After clarification by centrifugation at 3000 × *g*, the maintenance medium containing ^{32}P-labeled Clone 13 virus was precipitated by PEG 6000 (7 g/100 ml) in the presence of NaCl (2.3 g/100 ml) for 4 h at 4 °C and centrifuged at 10,000 × *g* for 40 min. The pelleted virus was resuspended in STE (20 mM Tris–HCl pH 7.4, 100 mM NaCl and 1 mM EDTA) and RNA extracted with Trizol reagent LS (Invitrogen), according to manufacturer's recommendations. After denaturation for 1 h at 50 °C in a buffer containing 1 M glyoxal (Merck), 50% (vol/vol) DMSO and 10 mM of MOPS buffer, the RNAs were electrophoresed in a 1.4% agarose gel (McMaster and Carmichael, 1977). Electrophoresis was performed at 50 V in MOPS buffer (20 mM 3-[*N*-Morpholino]-propane-sulfonic acid, 5 mM Na acetate, 1 mM EDTA pH 7.0). The gel was dried at 60 °C and exposed on an X-ray film at −80 °C.

Analysis of ^{32}P-labeled cytoplasmic viral RNAs

Thirty minutes before infection, 10-mm dishes of confluent BHK21 cells were incubated with actinomycin D (2 µg/ml). Cells were infected with Clone 13 RVFV strain at an MOI of 1 or mock infected. [^{32}P]phosphoric acid (20 µCi/ml) was then added to the medium 30 min after infection until 7.5 h post-infection. At that time, total cellular RNA was extracted by Trizol reagent (Invitrogen) and analyzed as described above for viral RNAs.

Northern blot analysis

Total cellular RNAs were extracted 24 h post-transfection by Trizol reagent. Four micrograms of total RNA was separated in 1.4% agarose after denaturation with glyoxal and transferred onto Hybond-N membranes (Amersham Pharmacia Biotec). Blots were prehybridized for 2 h at 65 °C in a solution containing 50% formamide, 5× SSPE (1× SSPE: 0.18 M NaCl, 10 mM NaH_2PO_4 and 1 mM EDTA) (pH 7.0), 5× Denhardt solution, 0.5% SDS, 2 µg per ml of boiled salmon sperm DNA. ^{32}P-labeled riboprobes were then added to the hybridization tube and incubated for 18 h at 65 °C. Membranes were washed successively with 2× SSPE, 0.1% SDS twice for 10 min each at

room temperature followed by 1× SSPE, 0.1% SDS at 65 °C and by 0.1× SSPE, 0.1% SDS at 65 °C for 10 min. Membranes were exposed to intensifying screen and revealed with STORM 820 apparatus (Molecular Dynamics).

CAT riboprobes were synthesized by in vitro transcription of $pT7CAT_{AK}$, a pGEM-based plasmid containing the CAT ORF already described (Kohl et al., 1999a), using SP6 or T7 polymerase and [$\alpha-^{32}$P]CTP (3000 Ci/mmol, Amersham). This plasmid contains the CAT ORF between the SP6 and T7 promoters into pGEM-4Z vector at the HindIII site of the polylinker.

Acknowledgments

This study was supported by grants from the Pasteur Institute to MB and from NIH Grant no. U01 AI066327-01 to R.F. and M.B. N.G. was supported by a "Contrat Jeune Chercheur" from Délégation Générale à l'Armenent (DGA) and a fellowship from Académie de Médecine and Fondation Odette and Jean Duranton de Magny.

References

Anonymous, 2000a. Outbreak of Rift Valley fever, Yemen, August–October 2000. Wkly. Epidemiol Rec. 75 (48), 392–395.

Anonymous, 2000b. Rift Valley fever, Saudi Arabia, August–October 2000. Wkly. Epidemiol Rec. 75 (46), 370–371.

Barr, J.N., Wertz, G.W., 2004. Bunyamwera *Bunyavirus* RNA synthesis requires cooperation of 3′- and 5′-terminal sequences. J. Virol. 78 (3), 1129–1138.

Barr, J.N., Elliott, R.M., Dunn, E.F., Wertz, G.W., 2003. Segment-specific terminal sequences of Bunyamwera *Bunyavirus* regulate genome replication. Virology 311 (2), 326–338.

Bishop, D.H., Gay, M.E., Matsuoko, Y., 1983. Nonviral heterogeneous sequences are present at the 5′ ends of one species of snowshoe hare *Bunyavirus* S complementary RNA. Nucleic Acids Res. 11 (18), 6409–6418.

Bouloy, M., Plotch, S.J., Krug, R.M., 1978. Globin mRNAs are primers for the transcription of influenza viral RNA in vitro. Proc. Natl. Acad. Sci. U.S.A. 75 (10), 4886–4890.

Collett, M.S., 1986. Messenger RNA of the M segment RNA of Rift Valley fever virus. Virology 151 (1), 151–156.

Elliott, R.M., 1996. In: E.R.M. (Ed.), The Bunyaviridae. Plenum Press, New York.

Elliott, R.M., Bouloy, M., Calisher, C.H., Goldbach, R., Moyer, J.T., Nichol, S.T., Pettersson, R.F., Plyusnin, A., Schmaljohn, C.S., 2000. Family Bunyaviridae. In: Van Regenmortel, M.H.V., Fauquet, C.M., Bishop, D.H.L., Cartens, E.B., Estes, M.K., Lemon, S.M., Maniloff, J., Mayo, M.A., McGeoch, D.J., Pringle, C.R., Wickner, R.B. (Eds.), Virus Taxonomy. Classification and Nomenclature of Viruses. Seventh Report of the International Committee on Taxonomy of Viruses. Academic, San Diego, pp. 614–616.

Elroy-Stein, O., Fuerst, T.R., Moss, B., 1989. Cap-independent translation of mRNA conferred by encephalomyocarditis virus 5′ sequence improves the performance of the vaccinia virus/bacteriophage T7 hybrid expression system. Proc. Natl. Acad. Sci. U.S.A. 86 (16), 6126–6130.

Flick, R., Pettersson, R.F., 2001. Reverse genetics system for Uukuniemi virus (Bunyaviridae): RNA polymerase I-catalyzed expression of chimeric viral RNAs. J. Virol. 75 (4), 1643–1655.

Flick, K., Hooper, J.W., Schmaljohn, C.S., Pettersson, R.F., Feldmann, H., Flick, R., 2003a. Rescue of Hantaan virus minigenomes. Virology 306 (2), 219–224.

Flick, R., Flick, K., Feldmann, H., Elgh, F., 2003b. Reverse genetics for Crimean-Congo hemorrhagic fever virus. J. Virol. 77 (10), 5997–6006.

Flick, K., Katz, A., Overby, A., Feldmann, H., Pettersson, R.F., Flick, R., 2004. Functional analysis of the noncoding regions of the Uukuniemi virus (Bunyaviridae) RNA segments. J. Virol. 78 (21), 11726–11738.

Gerdes, G.H., 2002. Rift Valley fever. Vet. Clin. North Am., Food Anim. Pract. 18 (3), 549–555.

Giorgi, C., 1996. Molecular biology of *Phlebovirus*. In: Elliot, R.M. (Ed.), The Bunyaviridae. Plenum Press, New York, NY.

Giorgi, C., Accardi, L., Nicoletti, L., Gro, M.C., Takehara, K., Hilditch, C., Morikawa, S., Bishop, D.H., 1991. Sequences and coding strategies of the S RNAs of Toscana and Rift Valley fever viruses compared to those of Punta Toro, Sicilian Sandfly fever, and Uukuniemi viruses. Virology 180 (2), 738–753.

Hutchinson, K.L., Peters, C.J., Nichol, S.T., 1996. Sin Nombre virus mRNA synthesis. Virology 224 (1), 139–149.

Ikegami, T., Peters, C.J., Makino, S., 2005a. Rift valley fever virus nonstructural protein NSs promotes viral RNA replication and transcription in a minigenome system. J. Virol. 79 (9), 5606–5615.

Ikegami, T., Won, S., Peters, C.J., Makino, S., 2005b. Rift Valley fever virus NSs mRNA is transcribed from an incoming anti-viral-sense S RNA segment. J. Virol. 79 (18), 12106–12111.

Kohl, A., Billecocq, A., Prehaud, C., Yadani, F.Z., Bouloy, M., 1999a. Transient gene expression in mammalian and mosquito cells using a recombinant Semliki Forest virus expressing T7 RNA polymerase. Appl. Microbiol. Biotechnol. 53 (1), 51–56.

Kohl, A., Bridgen, A., Dunn, E., Barr, J.N., Elliott, R.M., 2003. Effects of a point mutation in the 3′ end of the S genome segment of naturally occurring and engineered Bunyamwera viruses. J. Gen. Virol. 84 (Pt 4), 789–793.

Kohl, A., Dunn, E.F., Lowen, A.C., Elliott, R.M., 2004a. Complementarity, sequence and structural elements within the 3′ and 5′ non-coding regions of the Bunyamwera orthobunyavirus S segment determine promoter strength. J. Gen. Virol. 85 (Pt 11), 3269–3278.

Kohl, A., Hart, T.J., Noonan, C., Royall, E., Roberts, L.O., Elliott, R.M., 2004b. A Bunyamwera virus minireplicon system in mosquito cells. J. Virol. 78 (11), 5679–5685.

Kozak, M., 2002. Pushing the limits of the scanning mechanism for initiation of translation. Gene 299 (1–2), 1–34.

Krug, R.M., 1981. Priming of influenza viral RNA transcription by capped heterologous RNAs. Curr. Top. Microbiol. Immunol. 93, 125–149.

Li, M.L., Ramirez, B.C., Krug, R.M., 1998. RNA-dependent activation of primer RNA production by influenza virus polymerase: different regions of the same protein subunit constitute the two required RNA-binding sites. EMBO J. 17 (19), 5844–5852.

Linthicum, K.J., Anyamba, A., Tucker, C.J., Kelley, P.W., Myers, M.F., Peters, C.J., 1999. Climate and satellite indicators to forecast Rift Valley fever epidemics in Kenya. Science 285 (5426), 397–400.

Lopez, N., Muller, R., Prehaud, C., Bouloy, M., 1995. The L protein of Rift Valley fever virus can rescue viral ribonucleoproteins and transcribe synthetic genome-like RNA molecules. J. Virol. 69 (7), 3972–3979.

Lowen, A.C., Elliott, R.M., 2005. Mutational analyses of the nonconserved sequences in the Bunyamwera Orthobunyavirus S segment untranslated regions. J. Virol. 79 (20), 12861–12870.

Lowen, A.C., Boyd, A., Fazakerley, J.K., Elliott, R.M., 2005. Attenuation of *Bunyavirus* replication by rearrangement of viral coding and noncoding sequences. J. Virol. 79 (11), 6940–6946.

McMaster, G.K., Carmichael, G.G., 1977. Analysis of single- and double-stranded nucleic acids on polyacrylamide and agarose gels by using glyoxal and acridine orange. Proc. Natl. Acad. Sci. U.S.A. 74 (11), 4835–4838.

Meegan, J.M., Peters, C.J., 1989. Rift Valley fever. In: Monath, T.P. (Ed.), The Arboviruses: Epidemiology and Ecology. IV CRC Press Inc, Boca Raton, FL.

Muller, R., Saluzzo, J.F., Lopez, N., Dreier, T., Turell, M., Smith, J., Bouloy, M., 1995. Characterization of Clone 13, a naturally attenuated avirulent isolate of Rift Valley fever virus, which is altered in the small segment. Am. J. Trop. Med. Hyg. 53 (4), 405–411.

Neumann, G., Zobel, A., Hobom, G., 1994. RNA polymerase I-mediated expression of influenza viral RNA molecules. Virology 202 (1), 477–479.

Patterson, J.L., Kolakofsky, D., 1984. Characterization of La Crosse virus small-genome transcripts. J. Virol. 49 (3), 680–685.

Pettersson, R.F., Hewlett, M.J., Baltimore, D., Coffin, J.M., 1977. The genome

of Uukuniemi virus consists of three unique RNA segments. Cell 11 (1), 51–63.

Radecke, F., Spielhofer, P., Schneider, H., Kaelin, K., Huber, M., Dotsch, C., Christiansen, G., Billeter, M.A., 1995. Rescue of measles viruses from cloned DNA. EMBO J. 14 (23), 5773–5784.

Rossier, C., Raju, R., Kolakofsky, D., 1988. LaCrosse virus gene expression in mammalian and mosquito cells. Virology 165 (2), 539–548.

Schmaljohn, C., Hooper, J.W., 2001. Bunyaviridae: the viruses and their replication. In: Fields, B.N., Knipe, D.M. (Eds.), Fields Virology, 2.2 vols. Lippincott Williams & Wilkins, Philadelphia.

Swanepoel, R., Coetzer, J., 1994. Rift Valley fever. In: Coetzer, J., Thompson, G., Tustin, R. (Eds.), Infectious Diseases of Livestock with Special Reference to Southern Africa. Oxford University Press, South Africa, Cape Town.

Zobel, A., Neumann, G., Hobom, G., 1993. RNA polymerase I catalysed transcription of insert viral cDNA. Nucleic Acids Res. 21 (16), 3607–3614.

Zucker, M., Mathews, D.H., Turner, D.H., 1999. Algorithms and Thermodynamics for RNA Secondary Structure Prediction: A Practical Guide. Kluwer Academic Publishing, Dordrecht, The Netherlands.